Reply to Referee #1

We are grateful to the Referee for attention and inspiring us to make a deeper insight in plasma physics.

Comment
The previous version of the paper did not reach any substantial conclusions. This version of the paper does not reach any substantial conclusions either. It seems that the authors do not realize that simple description of observations is not physics. It is necessary to extract new knowledge from these observations. I inclined to reject the paper. Yet, I would like to give one more chance. Please make sure to show how this study advances our understanding of shock physics beyond just presenting figures and stating that "Magnetic field and ion density jumps are smeared to a couple tens of seconds". Claiming that "High-ß ($\beta > 10$) shocks are relatively rare and largely unexplored class of Earth bow shock" is inappropriate for Conclusions. What new physics is found ?

Reply
Perhaps, the referee is not satisfied with the style of Conclusions section. We are aware of three papers addressing specifically high-beta shocks (Formisano et al, 1975, Winterhalter et al, 1988, Farris et al, 1992). In order to clarify our advances we now include a more detailed description of previous results in Introduction. Our new quantitative results are actually fully listed in subsection 3.4.
1. First of all, the study systematically addresses the issue of finding high-beta shock examples and proving their beta values. The overall number of potential candidates is estimated. Statistics of Cluster multipoint shock events with small separation is assembled.
2. With 22 Cluster examples, a typical appearance of oblique high-beta shock was well identified, including ramp structure and general properties of variations.
3. Polarization, typical frequency, in some cases, the spatial scale of dominating magnetic variations was determined. Two distinct variants of wave structure were found, with dominating 0.5 Hz and 2 Hz waves. (Note, that the only wave property reported before was "very high amplitude").
4. Comparison with the previous results shows distinct difference of observed variations from that previously reported in low beta shocks, in particular, it is not consistent with fast magnetosonic or Alfven waves. There is some consistency with Weibel mode.
What was really not done, is some "ultimate identification of wavemode", requiring reliable wave vector determination. It, of course, remains one of our primary goals in the following studies. Perhaps this was meant by the Referee as *absence of physics*. We, however, can not expect that all problems of high-beta shocks will be solved in the first paper. Hundreds of papers were written on more ordinary shocks, and still many things are not clear. We make the conclusions more specific and also enhance interpretations (though more speculative at this stage) in Discussion.

Replies to Referee #2.

We would like to thank the Referee for the attentive reading and several useful suggestions.

Comment

The paper is about magnetic fluctuations in the Earth's high-beta bow shock. The authors combine data from the Cluster spacecraft and the OMNI database. The topic of high-beta shocks is highly interesting because of their application to astrophysical shocks. The language in the paper is mostly fluent and clear. The data analysis is detailed and largely precise. However, the presentation of the data is at times lacking and the analysis is sometimes incomplete. The conclusions mentioned in the paper are that the shock ramp are smeared to 10s of seconds due to the magnetic fluctuations and a somewhat quantitative description of the wave properties of the fluctuations.

I am inclined to consider these conclusions not sufficient to advance our understanding of high-beta shocks and how the fluctuations are different from those in other shocks. The authors should strive to at least qualitatively describe how the high-beta shock fluctuations differ from "normal" shocks and attempt to measure the spatial extent of the fluctuations. The authors should also more carefully try to validate the OMNI values of beta with the Cluster measurements.

Reply

We should first mention, that up to now observational information on high-beta shocks was very limited (mostly three papers: Formisano et al, 1975, Winterhalter et al, 1988, Farris et al, 1992). The wave analysis was not performed at all. These papers only checked some very general shock parameters and noted presence of high-amplitude turbulence (in comparison with lower-beta shocks). In order to clarify this issue, we now include a more detailed description of previous results in Introduction. We do not count here several reports addressing beta=2 shocks as high-beta ones (like Scudder et al, 1986). Therefore, we consider, that our study in fact makes a significant advance for high-beta shocks:

1. First of all, the study systematically addresses the issue of finding high-beta shock examples and proving their beta values. This issue was not addressed at all in the first publications. The overall number of potential candidates is estimated. Statistics of Cluster multipoint shock events with small separation is assembled.

2. With 22 Cluster examples, a typical appearance of oblique high-beta shock was well identified, including ramp structure and general properties of variations.

3. Polarization, typical frequency, in some cases, the spatial scale of dominating magnetic variations was determined. Two distinct variants of wave structure were found, with dominating 0.5 Hz and 2 Hz waves. (Note, that the only wave property reported before was "very high amplitude").

4. Comparison with the previous results shows distinct difference of observed variations from that previously reported in some types of low beta shocks, in particular, it is not consistent with fast magnetosonic or Alfven waves. There is some consistency with Weibel mode.

What was really not done, is some "ultimate identification of wavemode", requiring reliable wave vector determination. It, of course, remains one of our primary goals in the following studies.

We intentionally do not directly and systematically compare with lower beta shocks examples and statistics. Simply we cannot avoid comparing with the some well-known types of shocks (for example, whistlers and ramp structures at q-perp supercritical shock). We also briefly list some previous results on downstream waves which are rather disordered. This is done for two reasons:

1. We are not interested so much in finding **the specific list of differences** with lower beta shocks, it is only one of possible approaches to the subject. We are interested in determining properties of high-

beta shocks as such, having in mind their cross-discipline importance. In fact, the larger is beta, more interesting is the study. We just cannot avoid comparing with the some well-known types of shocks (for example, whistlers at q-perp supercritical shock). We now state this aspect more carefully in Discussion and Concusions.

2. There exist thousands of crossings of low-beta shocks with very diverse properties. References in our report partially illustrate this diversity of conclusions about fluctuation modes and ramp structure. The only well bounded classes are supercritical q-perp shocks with domination of whistler mode fluctuations and q-par shocks. Beyond these two classes, it is totally unclear, which low-beta shocks to choose for comparison. Proper selection of low beta examples would be more laborious, than this study of high-beta events.

Thus we consider, that inclusion of additional low-beta examples will strongly deviate us from the main goal. We rechecked our wording in Abstract and Conclusions to avoid misunderstanding.

Issue of validation of OMNI beta values is addressed below among more specific comments. We also added estimates of shock speed, spatial length of ramp.

WHISPER density was used to further validate local beta. However, difficulties with local ion temperature do not allow to ultimately conclude the validation.

We also reworded Discussion and Conclusions to make them more specific, to include more interpretation specific to high-beta shocks.

***

Comment:

Page 2, Line 30: The authors should specify how the Geotail, THEMIS, and Interball data were used in this study. This is as far as I can see the last mention of these missions. This paragraph appears out of place. Such a detailed description of the data used is probably better in the next section.

Reply:

OK. Data description paragrpahs were moved to Section 2. Mention of "Geotail, THEMIS, and Interball" is deleted, since it appears to be confusing. These spacecraft were used to understand the shock statistics during the whole analyzed period 1995-2017, but in this study only Cluster multipoint examples are presented.

***

Comment:

Page 3, Line ~3: Motivate why Cluster data was not used directly to calculate beta. Specifically why CIS-HIA/CODIF was not used for density/temperature of the solar wind.

Reply:

HIA/CODIF data were not used to calculate local beta for two reasons. (1) Presence of even a small number of reflected ions strongly changes upstream temperature. (2) OMNI ion data are provided by dedicated solar wind instruments (retarding analyzers), while HIA/CODIF are general-purpose deflecting spectrometers. The latter are not suited to measure reliably tiny solar wind ion temperature. Considering validity of Cluster solar wind density and temperature goes far beyond purpose of this paper. Since in the solar wind magnetic field is more variable than density, we consider it is more reliable to use verified OMNI beta data and recheck comparing Cluster and OMNI magnetic field as explained in the paper. However, we now included WHISPER density data, where available (in two cases), for illustration, they fit well with OMNI density

****

Comment:

Page 3, Line 5: The authors should clarify what the constant values in OMNI are and how that might affect the validity of the reported beta value.

Reply:

This information is added in sec 2 and sec. 4.1. These values are multiyear averages, deviation from them may slightly modify actual beta. Among other problems with beta, this source of errors is not the primary one.

(in Sec.2): β values are precalculated in OMNI-2, assuming constant electron temperature (140000 K), He++ fraction (0.05) and He++ temperature (four times larger than proton temperature).

(In Sec.4): Assumptions on the constant helium content and constant electron temperature, used while OMNI β calculations may also result in some errors. For example, a factor of two change in electron temperature will result in the change of β by about 30\%. Factor of two variations of the He++ content will result in variations of β around 10\%.

****

Comment:

Page 3, Line 24: The figure referred to is Fig 4.

Reply:

Thanks, corrected

****

Comment:

Page 3, Line 25: "The scatter is indeed large." Include a discussion about why and what it means for the results of the study. Also specify which data were used when both were available. ACE or WIND?

Reply:

OMNI data were always used. We improved description of statistics. Right in the next paragraph it is stated (*what it means for the results?*), that local beta confirmation is always necessary. Full discussion is already included in the relevant section.

Now in Sec 2: Fig. 4 shows comparison of β calculation for Wind and ACE 1-hour data (only for times, when Wind data were used in OMNI).For this OMNI-2 subset there were 618 1-hour points, with $\beta>$10 either in Wind or ACE data. Only for 196 of them difference between β at two spacecraft was less than 30\%. For more than half of events (318) difference between the spacecraft was larger than 50\%. Such substantial difference is partially due to quadratic dependence of β on magnetic field.

****

Comment:

Figure 6: - Panel b: Plots of magnitudes should contain the value 0.

Reply:

This depends on the scope of change in the variable. We included "zero" everywhere, where reasonable. Updated Figures are 6, S1, S3.

****

Comment:

- Panel c: The authors should explain why the temperature appears to fall over the shock when the primary role of a shock is to heat the plasma. Also explain why the parallel temperature is larger than perpendicular in the shock foot.

Reply:

We changed the scale of temperature plot to logarithmic one. Perpendicular temperature steadily grows across the transition. Parallel temperature maximizes right upstream the shock, because of the presence of upstream-moving ions (probably mostly field-aligned). The spread of velocity between solar wind flow and these ions creates a false increase of ion parallel temperature.

(in Sec. 3.1): Cluster ion (proton) density in solar wind is lower, than that in OMNI, however WHISPER electron density is almost the same. Proton perpendicular temperature grows as expected towards downstream, while the parallel temperature peaks just upstream the shock front. We attribute this peak to the upstream-moving field-aligned protons. The presence of two populations in the distribution function with strongly different flow velocity, results in the false temperature increase.

****

Comment:

-Panel e: Something seems to be wrong with the ion energy here (even more clear in the supplement). The solar wind speed: 250 km/s -> proton energy: 330 eV -> should be on line between 10ˆ2 and 10ˆ3 which is ~320 eV. But the solar wind is even below 10ˆ2 eV. This must be wrong.

Reply:

Ok. Thanks a lot! Energy values were twice subjected to logarithm by mistake. Now corrected. Updated figures are attached in the end of this text.

****

Comment:

Page 7, Line ~5: I think there is a missed opportunity to determine the shock speed here. It could put a number on shock extent in space, and not just time. There are several ways to calculate shock speed with one spacecraft, see the ISSI book " Analysis Methods for Multi-Spacecraft Data" chapter 10. Also, Cluster 2 encounters the same shock~1min later. This could be used in a timing analysis.

Reply:

OK, thanks for the idea! Indeed, this will provide some additional information. Cluster 2 crosses the shock within two minutes. However, such determination of shock speed is not very reliable quantitatively. Nonetheless we include this information in the text.

As concerns single spacecraft methods, they returned very differing results for the shock speed around 100 km/s. In fact, it is not surprising. These formulas manipulate with velocity of the order of hundreds km/s to get the result of the order of ten km/s. With noisy data, computations of such kind are prone to errors and seldom used. Thus we choose not to include these estimates.

Changes in the text:

(In Sec 3.1): However, Cluster 2, being about 6000 km away from the pair C3 and C4, crossed the shock two minutes later (exact values are 6231 km and 124 s between C3 and C2, not shown here). The separation along the model normal is 1032 km, the spacecraft are placed almost along the shock front. Shock velocity along the normal is then 8.3 km/s outbound. This calculation is not very reliable for two reasons: (1) The spacecraft are mostly separated along the front by about 6000 km, shock motion may be different in two so different points. (2) The reverse crossings occurred less than 10 min later, thus shock speed might substantially change on a scale of two min (separation between C3 and C2). Nevertheless, one can estimate the spatial scale of the smeared ramp. Duration of 35 s corresponds to 290 km. The gyroradius of solar wind proton is $\sim$700 km, proton inertial scale is $\sim$80 km.

(In sec 3.2): Similar to Example 1, one can estimate shock speed along the normal, comparing with C2 crossings (not shown here). However for this example, the spacecraft separation is more than 11000 km, while the separation along the model normal is much smaller, just about 100 km. The estimated shock speed is 1.5--2.2 km/s (comparing the pairs C3-C3 and C4-C2), corresponding to the smeared ramp width about 50 km. However, this estimate is very unreliable, since the calculation result would strongly depend on small variations of the actual normal.

(In Sec 3.3): Similar to Example 1, one can estimate shock speed along the normal, comparing with C2 crossing (not shown here). The spacecraft separation is 5700--5800 km, while the separation along the model normal is about 1400 km. The estimated shock speed is about 11 km/s, corresponding to the smeared ramp width about 330 km. The gyroradius of solar wind proton is about 2000 km, due to very low IMF, proton inertial scale is $\sim$80 km.

(In Discussion): For example the main magnetic and ion density increase in the shock front was for all observed event around always several tens of seconds or several hundred km for typical shock proper velocity of about 10 km/s. This scale is larger, than proton inertial length, but smaller than ion gyroradius in solar wind. Dependence of shock spatial scale on β is an interesting moment and should be addressed in future studies on larger statistics.

***

Comment:

Page 10, Last paragraph: I think the statement "minimum variance (nominal propagation) direction is well defined" is a bit strong considering the eigenvalue ratio is as big as 0.5.

Reply:

Here the intermediate-to-maximum ratio is 0.5, while the minimum-to-intermediate ratio, defining quality of the minvar, is small enough - 0.15. So, the statement is correct.

***

Comment:

Page 10, Last paragraph: "The time shift between the magnetic measurements along the maximum variance component is 0.22" It seems that the two time series (Fig 10b) are quite different. The authors should discuss how this might affect the certainty of the timing.

Reply:

We apply the correlation analysis on a small interval 160115-160125 only, since indeed on other intervals the differences are large. On the given interval the large-scale lower-frequency structures are similar, while the most of differences are due to higher-frequency and lower-amplitude variations. In fact, this issue is mentioned in the very beginning of description, since this example was chosen to show a case with substantial difference of magnetic variations.

Change in the text:

(In Section 3.2): The specific feature of this event is a difference of C3 and C4 oscillations during the first 20 \unit{s} downstream the front (16:01:25--16:01:35 UT), despite relatively small separation. The substantial difference in waveforms remains also further downstream. The presence of such difference in amplitudes is typical for all shocks registered during this day (8 crossings within 2 hours in Table S1). Despite the differences, it is possible to perform multipoint separation analysis for the interval 16:01:15-16:01:25, where two waveforms in B_y component (Fig. 10b) are kind of similar and shifted by a fraction of period.

(In Section 4.3): The second variant of a spatial scale is illustrated with Example 2. It includes the mix of scales of the order of hundred \unit{km}, which can be captured with our spacecraft separation, and of the order of tens \unit{km}. As a result, the waveforms are rather different, but common features can sometimes be traced. Finally, the third variant (Example 3) suggests the dominating spatial scale of at most 200 \unit{km}.

****

Comment:

Figure 13: Legends for C3, C4 are missing.

Reply: OK, corrected.

****

Comment:

Page 19, Line 13: "The ramp is often used to determine the shock motion with multipoint measurements, but in our case it is impossible". This is not true. With only C3 and C4 it is impossible but in at least one case there is another Cluster satellite that could potentially be used.

Reply:

Determination of shock velocity is commented above. Here, we would like to insist, that the ramp can not be used to determine the scale with C3-C4 timing. With C2-C3 or C2-C4 timing the detailed form of ramp is unimportant, since the time difference is large (2 min), so even completely different form of the main jump (within couple of seconds) will not affect the computational result.

****

Comment:

Page 19, Line 27: Thus observed variations are strongly different from that in low-beta supercritical events ..." This appears to me to be a strong conclusion. Why is this not mentioned in "Conclusions"?

Page 19, Line 29: "Observed polarization is also not consistent with the earlier suggested alfven mode" also appears to be a strong conclusion. Also it is: "Alfvén".

Reply:

See general comment in the beginning. Conclusions are now reformulated. We state, that the observed variations are not alike those previously reported for some low-beta shocks.

****

Comment:

Page 20, Line 21: "Magnetic field and ion density jumps are smeared to a couple tens of seconds" This is a very imprecise statement. It is completely possible for even low beta quasi-perp shocks to be so slow that the ramp is smeared to minutes. An attempt to measure the shock ramp in kilometers instead of seconds would be desirable.

Reply:

Done. See reply above.

****

Comment:

Figure S1: - Caption says C4. C4 does not have a functioning CIS-HIA. It should say C3? - Panel b: The OMNI density appears to not match the CIS-HIA density. The authors should try to validate the density with some other instrument, like CIS-CODIF or WHISPER. - Same comment about ion energy in spectrograms.

Figure S3: Same comments as Fig S1.

Reply:

OK. This is a misprint in captions of S1 and S3. Example 1 uses C4 CODIF, Example 2 and 3 – C3 HIA as written on spectrograms.

Solar wind density is not a strong side of Cluster measurements. We rechecked with WHISPER electron density, it is closer to OMNI, than ion density, however we do not use local density for any quantitative conclusions. Corrected Figures are 6, S1 and S3

******

Comment:

There are also some minor language errors that I have not listed. Watch out for missing or superfluous "the" as well as the difference between "its" and "it's".

Reply:

Done as we can find.

Low frequency magnetic variations at high-β Earth bow shocks

Anatoli A. Petrukovich[1], Olga M. Chugunova[1], and Pavel I. Shustov[1]

[1]Space Research Institute of Russian Academy of Sciences, Moscow, Russia

Correspondence: A.A.Petrukovich (a.petrukovich@cosmos.ru)

Abstract. Earth's bow shock in high β (ratio of thermal to magnetic pressure) solar wind environment is a rare phenomenon. However such an object is ubiquitous in astrophysical plasmas. Typical solar wind parameters related with high β (here $\beta > 10$) are: low speed, high density and very low IMF 1–2 nT. These conditions are usually quite transient and need to be verified immediately upstream of the observed shock crossings. About a hundred high-β shocks were initially identified during 1995–2016 mostly with oblique or quasi-perpendicular geometry and high Mach number. In this report 22 crossings by Cluster project are studied with multipoint analysis, allowing to determine spatial scales. **The main magnetic field and density increase is smeared to the length of couple tens of seconds (couple of hundred km). Dominating magnetic variations in the shock transition have amplitudes much larger than the background field and frequency of ~0.3–0.5 Hz (in some events — 1–2 Hz). This layout is quite characteristic for the studied shock type. Their polarization has no stable phase and is closer to linear, complicating determination of the wave propagation direction. Spatial scales of variations are within several tens to couple hundred km.**

Copyright statement. TEXT

1 Introduction

Shocks are the primary dissipation mechanism in space plasmas with supersonic flows (Sagdeev, 1966; Kennel et al., 1985; Krasnoselskikh et al., 2013). A brand new branch of plasma science, theory of collisionless shocks, appeared in the sixties, in response to new space observations. Solar wind forms bow shocks at planets and comets, as well as the termination shock at the heliospheric interface. Interplanetary shocks develop inside the heliosphere after solar eruptions, when large-scale transient structures propagate relative to the regular solar wind flow. In the distant space, shocks are associated with supernova explosions, stellar winds, collisions of galaxy clusters and are believed to have a leading role in the acceleration process of cosmic rays (Axford et al., 1977; Krymskii, 1977). Physics of space shocks was reviewed in AGU Geophysical Monographs, volumes 34 and 35 (1985). The Earth bow shock has been most thoroughly studied and is the main source of our in-situ knowledge of collisionless shock structure and dynamics.

Electromagnetic fields and waves in collisionless plasma shocks are of primary importance. Due to presence of magnetic field wide variety of shock types exists with quite differing structure (Kennel et al., 1985). Magnetic field vector enters

Rankine-Hugoniout equations, defining the relation between upstream and downstream conditions. In the absence of collisions, kinetic mechanisms of field-particle interactions are responsible for dissipation and particle acceleration (Sagdeev, 1966; Krasnoselskikh et al., 2013). With quasi-perpendicular shock geometry (when the angle between the shock normal and the upstream magnetic field is closer to 90°) ions cannot escape upstream and relatively sharp shock transition forms with

5 the ion-scale overall width (several thousand km). With quasi-parallel geometry (the angle is closer to 0°) ions easily escape upstream along magnetic field and shock transition smears to the scales around several Earth radii (Scudder et al., 1986; Burgess et al., 2005). Oblique shocks (angles around 45°) are in a sense intermediate in properties, when ions partially are capable to escape upstream, but generally have rather spatially localized transition similar to quasi-perpendicular ones.

Besides this large-scale magnetic field structure, also of interest at the Earth's bow shock are relatively low frequency mag-
10 netic variations (from one tenth to few Hz) with visually maximal amplitudes, which actually form the primary shock front structure, dissipating ions. For example, in a supercritical quasi-perpendicular shock, the oblique whistler waves near the lower-hybrid frequency ($\sim$5 Hz) form the magnetic ramp via the non-linear steepening and decay cycle (Krasnoselskikh et al., 2002, and references therein). In the several studies the wavelength of these waves and the scale of shock ramp were determined to be around 10-s of km and oscillations were in fact identified as whistlers (Petrukovich et al., 1998; Walker et al.,
15 2004; Hobara et al., 2010; Schwartz et al., 2011; Dimmock et al., 2013; Krasnoselskikh et al., 2013). Cyclic shock reformation is typical also for quasi-parallel shocks with substructures known as SLAMS and oblique shocks (Lefebvre et al., 2009). Specifics of a plasma wave mode, driving the front reformation, depends of local plasma parameters, Mach number, etc. Immediately downstream of the shock front plasma waves at the frequencies below the ion cyclotron one were attributed to mirror, ion cyclotron, intermediate modes (e.g., Balikhin et al., 1997; Czaykowska et al., 2001). Yet one more issue of interest
20 is electron heating. It requires sufficiently small scale variations for non-adiabatic acceleration and following isotropisation (Balikhin et al., 1993; Vasko et al., 2018).

Of interest to some astrophysical applications are shocks in a weak magnetic field environment (high-β shocks), common in interstellar and intergalaxy space (e.g., Markevitch and Vikhlinin, 2007; Donnert et al., 2018). β is a dimensionless parameter, a ratio of plasma thermal to magnetic energy density. For low background magnetic fields, shock-associated variations
25 may be also considered as kind of 'magnetic field amplification', increasingly important for particle heating. Unfortunately, observations of high β shocks near Earth are quite rare, since the solar wind plasma usually has $\beta \sim 1$.

In our study we take $\beta > 10$ as threshold of high β, this choice is explained further below. Very few investigations of high-β shocks were published. Coroniti (1970) in a theoretical study suggested Alfvén mode to dominate downstream such a shock. Formisano et al. (1975) presented three cases of OGO-5 spacecraft observations with β equal to 8, 170, 49.
30 **General layout of these crossings was discussed and large magnetic field excursions up to 20 times larger than IMF were reported. Presence of some transient 'precursor activations' upstream of the main transitions was interpreted as a sign of principal nonstationarity of a shock structure. It was concluded, that despite formal high β, magnetic field should not be ignored in theory studies s of shock structure. Winterhalter and Kivelson (1988) stated that high-amplitude magnetic variations, which are larger than the main magnetic jump, are typical for the cases with higher β. However**
35 **specific examples of interest to our study were not shown. Farris et al. (1992) investigated one shock with β equal to 18,**

checking validity of Rankine-Hugoniot conditions and also mentioning high-amplitude magnetic variations. However, neither of these studies studied in detail these variations at shock transition zone. Finally, we also note, that in some, rather numerous, investigations moderate $\beta \geq 1$ was termed as "high-β" regime (e.g., $\beta = 2.4$ in Scudder et al., 1986).

We perform an extended experimental study of high-β bow shocks, with a first, to the best of our knowledge, multi-point analysis of dominating low-frequency magnetic varations at high-β shock transition using observations of Cluster project. To access possible solar wind variability we use also ACE and Wind final Earth-shifted data from OMNI-2 archive. Though such solar wind statistics is generally known (review in Wilson et al., 2018), some issues relevant to shock identification and analysis are still worth addressing. All vectors are in GSE frame of reference.

2 Solar wind statistics and details of search procedure

We use 1-hour OMNI-2 data for the period 1995–2017 to determine occurrence of high β solar wind for the subsequent shock analysis. β **values are precalculated in OMNI-2, assuming constant electron temperature (140000 K), He++ fraction (0.05) and He++ temperature (four times larger than proton temperature).** The average solar wind β is somewhat larger than unity. High β conditions are unevenly distributed across solar cycles (Fig. 1), being more frequent at the solar minima 1996–1997 and 2007–2009. For the threshold $\beta > 10$ there are 50–500 hours per year, while for $\beta > 20$, the number is about 3–5 times smaller.

Figure 2 shows distributions of magnetic field magnitude, solar wind speed, density and total static pressure for the full dataset of one-hour values during 1995–2017 and for the subset $\beta > 10$. High β corresponds to slow, cold and dense solar wind with low magnetic field (ion temperature not shown here). However the total static (magnetic plus thermal) pressure distribution is similar (Fig. 2b). Thus the high-β events are mostly depressions of magnetic field, compensated (at least on average) by increase of plasma density. The only notable difference of distributions for $\beta > 20$ (Fig. 2a, red line) is more frequent presence of magnetic field ~ 1 nT, with the average 1.6 nT, while for $\beta > 10$ the average is ~ 2.2 nT.

More than 50% of events with $\beta > 10$ have one-hour duration (one point in the analysed OMNI variant, not shown here). A sample event is in Fig. 3 (here 1-min OMNI-2 variant is used). There is about one-hour long decrease of magnetic field and density increase, corresponding to $\beta \sim 20$. At an occasional depletion of magnetic field below 2 nT β jumps to about 40–80 for few minutes. Since formation of high β conditions mostly depends on subtle variations of magnetic field magnitude around 1–2 nT (note, that β has square dependence on magnetic field), it should be quite sensitive to spatial inhomogeneity of solar wind and IMF, and, in particular, to differences between those detected at L1 (in OMNI dataset) and actually hitting Earth. **Fig. 4 shows comparison of β calculation for Wind and ACE 1-hour data (only for times, when Wind data were used in OMNI). The scatter is indeed large. For this OMNI-2 subset there were 618 1-hour points with $\beta > 10$ either in Wind or ACE data. Only for 196 of them difference between β at two spacecraft was less than 30%. For more than half of events (318) difference between the spacecraft was larger than 50%.**

We formulate several conclusions important for our specific shock analysis. (1). Solar wind intervals with high $\beta = 10$–20 are rare, but not extremely rare, and occur mostly during solar minimum. Thus some spacecraft (or the project phases with the
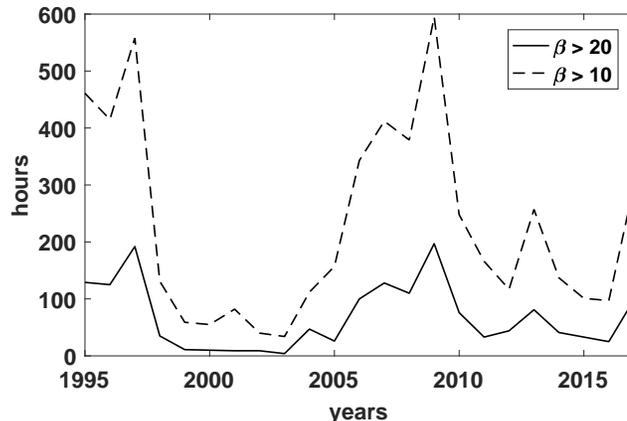
Figure 1. Number of hours with high β with respect to calendar year.

specific orbit or spacecraft separation) may almost completely miss such events. (2). Duration of intervals of interest is relatively short, thus selection of shocks with stable upstream conditions may be not always possible. (3). Very low interplanetary magnetic field, necessary for high-β events, is subject to strong (in relative terms) intrinsic spatial and temporal variability, thus actual β conditions and IMF vector need to be always rechecked with local measurements. This issue is further illustrated with the event selection results below and is elaborated more in Discussion.

Since the high-β shocks are rare, it is unreasonable to search for them, rechecking every registered event. It is more practical first to identify the intervals with the suitable conditions of solar wind. The semi-automated algorithm is used to assemble initial statistics of the shock candidates. For each 1-hour point in OMNI with $\beta > 10$, we check for possible spacecraft location within 5 R_E from the model bow shock (Farris et al., 1991). We scanned 1995–2017 observations by all available spacecraft. For this initial selection we use orbital data and spin-averaged magnetic field data from CDAWeb archive.

In a case any spacecraft is in the right place, the plots of solar wind, IMF, local magnetic field and plasma parameters are analyzed visually in the 5-hour window around the selected hour. These broad temporal and spatial spans are used to ensure that all possible crossings of a moving bow shock are captured for future analysis. Only events with the clear shock traversals (jumps in magnetic field and ion density) are accepted. Such a manual selection has definite bias to quasi-perpendicular and oblique shocks (which usually have a step-like appearance), but it is considered acceptable for this particular study. The most of these initially selected intervals actually contain no shock crossings.

Discovered particular shock crossings are checked with 1-min OMNI data. Plasma β is often below 10, either because registered shocks are just outside of initially selected hours, or because β varied on a time scale, smaller than an hour. Since a change of β is usually accompanied with the solar wind density change, there is a dynamic pressure change also. The latter drives large-scale shock motion and probability of shock registration by a spacecraft increases. In fact, many shock crossings are registered at a boundary of β change and such events are also discarded, since it is impossible to attribute them to stable upstream plasma conditions.
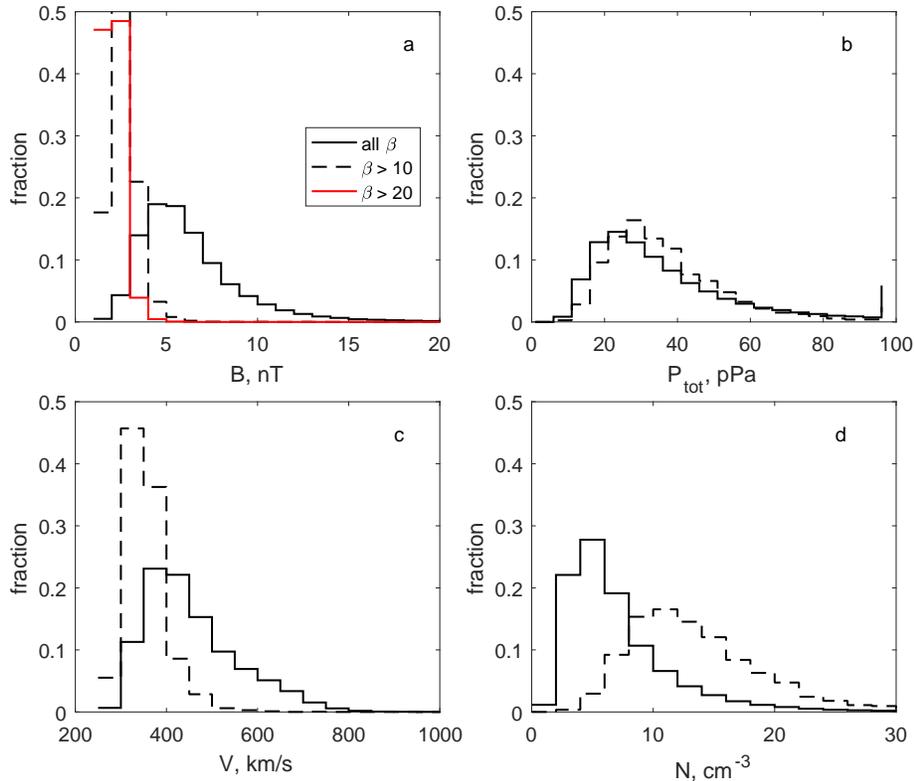
4

Figure 2. Histograms of solar wind and IMF occurrence for 1995–2017 (solid lines) and for $\beta > 10$ (dashed lines) subset. (a) Total magnetic field (red line corresponds to $\beta > 20$) , (b) total static pressure, (c) solar wind speed, (d) ion density.

10   Finally the list contained about a hundred individual crossings with average β about 20 (taken as 1-min OMNI value at the moment of shock front crossing). About ten events occurred with very high $\beta > 40$. The choice of initial threshold $\beta > 10$ (for 1-hour points) was finally justified at this stage, since a variant with initial $\beta > 20$ resulted with the almost empty list. However, all these events still need a more detailed confirmation, in particular, of local high β, stable enough crossing velocity, plasma data availability etc.

15   For the specific multipoint analysis in this investigation we selected 22 verified Cluster project crossings with relatively small spacecraft separation. The full list is in Table S1 in Supplement 1. **For the detailed analysis we used full-resolution Cluster FGM magnetic field (here with the sampling ~20 Hz) (Balogh et al., 2001) and HIA/CODIF ion data (sampling once in 8 seconds) (Rème et al., 2001) from Cluster Science Archive.** One event is from 2003, with the Cluster tetrahedron size of about 300 km, while the other are for the late years 2008–2016, when separation only between a pair of Cluster spacecraft C3 and C4 was controlled (30–150 km for our events). This uneven annual distribution is a consequence of the solar cycle dependence (Fig. 1). Events are grouped in 7 days. Specifically, 5 crossings are registered within one hour at December 18, 2011, 4 crossings — within two hours at January 3, 2008, 8 crossings — within two hours at January 4, 2008, 2 crossings
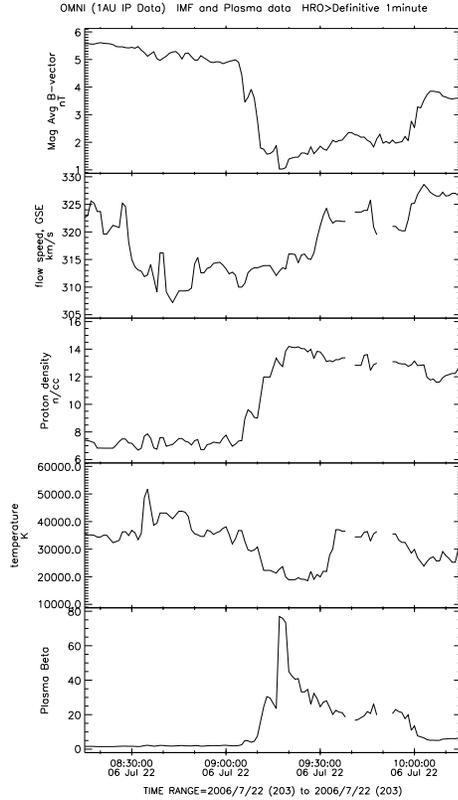
OMNI (1AU IP Data)   IMF and Plasma data   HRO>Definitive 1minute

TIME RANGE=2006/7/22 (203) to 2006/7/22 (203)

Figure 3. Example of high-β interval. From top to down: magnetic field magnitude, solar wind speed, proton density, proton temperature, plasma β. 1-min OMNI data set used.

— within one hour at February 16, 2012. However not all these adjacent crossings are similar. Some of these examples are presented below.

3   Shock examples

3.1   Event 1

The first example is registered by Cluster C3 and C4 spacecraft on 18 December 2011 (14:36–14:40 UT) with the separation 36 km. The spacecraft orbit is almost parallel to the model shock front (Fig. 5), but shock velocity is definitely much higher than the spacecraft velocity. Fig. 6 contains overview of magnetic field and plasma parameters. Solar wind speed is small $\sim$260 km/s, IMF magnitude — 2.5 nT (all characteristics are in Table S1). Alfvén Mach number is $\approx$18, magnetosonic Mach number is $\approx$5, β (according to 1-min OMNI) is 10.8.
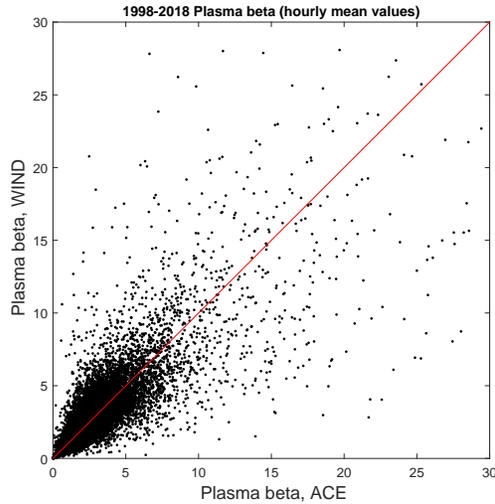
6

Figure 4. Comparison of Wind and ACE β using 1-hour data. See text for details. Red line is bisector

       Cluster ion (proton) density in solar wind is lower, than that in OMNI, however WHISPER electron density is almost

15   **the same. Proton perpendicular temperature grows as expected towards downstream, while the parallel temperature peaks just upstream the shock front. We attribute this peak to the upstream-moving field-aligned ions. Presence of two populations with strongly different flow velocity results in the false temperature increase. Thus using local ion data to calculate local β would be unreliable. We confirm β using local magnetic field only, since it is the most variable parameter (in comparison with the plasma density). Solar wind magnetic field measured locally by Cluster is the same**

20   **as OMNI data (compare two lines in Fig. 6d), therefore OMNI β value is confirmed. OMNI IMF vector direction is only $\sim 10^o$ different with the local upstream field taken at 14:40–14:41 UT (not shown here). The model shock normal angle with respect to OMNI (local) IMF θ_{Bn} is 46° (54°) (using Farris et al. (1991) model). The coplanarity calculation for the shock normal results in $\theta_{Bn} = 42^o$. Thus this is quasi-perpendicular or oblique supercritical bow shock with the reliably determined geometry. It's structure for more standard β is well studied (Scudder et al., 1986; Krasnoselskikh et al.,**

25   **2013; Lefebvre et al., 2009). The final value of downstream magnetic field is around 10 nT, and compression ratio is thus close to maximally possible value of 4, in accordance with the high Mach number.**

     The shock transition lasts about 200 seconds 14:37:00–14:40:30 from the first signs of gyrating ions upstream (Fig. 6f) up to the stable downstream conditions. The increase in magnetic field magnitude (aka shock ramp in a quasi-perpendicular case) is smeared within half a minute 14:37:45-14:38:20 UT and is accompanied with the similar smeared increase of ion density.

30   The nominal shock front transition is somewhat arbitrarily placed at 14:37:45 UT (marked by vertical line) at a first extended peak of magnetic field. The magnetic field increase is wavy, rather than regular or step-like, magnetic magnitude immediately downstream is often down to 5 nT. Thus it is impossible to determine the shock speed, comparing C3 and C4 measurements.

However, Cluster 2, being about 6000 km away from the pair C3 and C4, crossed the shock two minutes later (exact values are 6231 km and 124 s between C3 and C2, not shown here). The separation along the model normal is 1032 km, the spacecraft are placed almost along the shock front. Shock velocity along the normal is 8.3 km/s outbound. This calculation is not very reliable for two reasons: (1) The spacecraft are mostly separated along the front by about 6000 km, shock motion may be different in two so different points. (2) The reverse crossings occurred less than 10 min later, thus the shock speed might substantially change on a scale of two min (separation between C3 and C2). Nevertheless, one can estimate the spatial scale of the smeared ramp. Duration of 35 s corresponds to 290 km. The gyroradius of solar wind proton is ∼700 km, ion inertial length in solar wind is ∼80 km.

Despite the described smeared magnetic field increase, the full shock transition is rather compact and coherent and thus it is distinctly different from what expected for quasi-parallel shock with multiple shocklets (Burgess et al., 2005).

We highlight in Figure 7 the interval with the strongest low-frequency magnetic variations. Frequency spectra are in Figure 8. The magnetic profile is dominated by a variation with frequency around 0.3 Hz and amplitude up to 20 nT, more pronounced in B_y. An interval 14:37:27–14:37:47 is taken to estimate the wavelength. The main oscillation (0.3 Hz) is very similar at two spacecraft and visually the time shift between C3 and C4 is about a fraction of a second. Since the variation has a clear dominating frequency, it is more convenient to perform the time-domain multi-point analysis.

Parameters of magnetic variations, filtered in frequency range 0.1–0.77 Hz, are in Table 1. The vector of maximum variance is almost along local magnetic field (B_y component dominates), of minimum variance — along Z. Ratios of eigenvalues are $\lambda_{min}/\lambda_{int} = 0.34$, $\lambda_{int}/\lambda_{max} = 0.58$, and one may assume elliptic polarization. The time shift between magnetic measurements along the maximum variance component, determined with the correlation analysis, is 0.13 s. This value is rather reliably calculated, since it is 2–3 times larger than the sampling interval. The spacecraft separation along the minimum variance direction is 10 km and the resulting wavelength estimate is ∼250 km. However the hodograph of magnetic field rotation (Fig. 9) shows, that the polarization actually might be linear with the variable eigenvector (but mostly along the determined maximum variance). In such a case the propagation direction cannot be defined with the variance analysis. For the compressive low frequency MHD waves the propagation direction can be determined with the coplanarity approach (Hubert et al., 1998). The maximum variance direction, the magnetic field direction and the wavevector should be in the same plane. However, in our case, the angle between the maximum variance direction and the local magnetic field is rather small (only 12°) and coplanarity calculation result would be unrealiable.

We also estimate the span of principally possible wavelengths. The maximal one is ∼900 km, obtained taking full spacecraft separation 36 km. The Doppler shift is 0.04–0.58 Hz, depending on a wavelength and taken local proton velocity value (full 146 km/s or its projection to minimal eigenvector 41 km/s).

Finally we note the oscillations with higher frequency about 1 Hz and smaller amplitude of couple nT, which are best observable in B_z component (Fig. 7c and Fig. 8). The eigenvalue ratios (after filtering the frequency range 0.7–10 Hz) are $\lambda_{min}/\lambda_{int} = 0.68$, $\lambda_{int}/\lambda_{max} = 0.49$, thus reliable determination of any wave proper direction is definitely not possible. Oscillations are quite different at two spacecraft and the multipoint analysis also proved to be not possible.
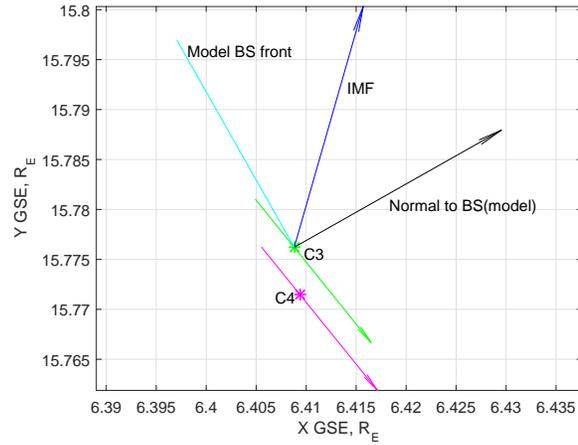
8

Figure 5. Spacecraft orbit and model shock position for shock 12 December 2011.

Table 1. Wave analysis data for shock 18 December 2011, 14:37:27–14:37:47.

max eigenvector, V_{max}	-0.23, 0.94, 0.27
med eigenvector, V_{med}	0.97, 0.20, 0.15
min eigenvector, V_{min}	-0.08, -0.29, 0.95
eigenvalues	2.23, 6.64, 11.50
magnetic field C3, B_3 (nT)	-3.58, 9.53, 0.96
local proton velocity C4 (km/s)	-118.1, 82.1, -29.29
angle, V_{max} and IMF	34°
angle, V_{min} and IMF	110°
angle, V_{max} and B_3	12°
angle, V_{min} and B_3	99°
peak frequency in max component	0.3 Hz
time shift in magnetic field along V_{max}	0.13 s
separation along V_{min}	10 km
wavelength	252 km
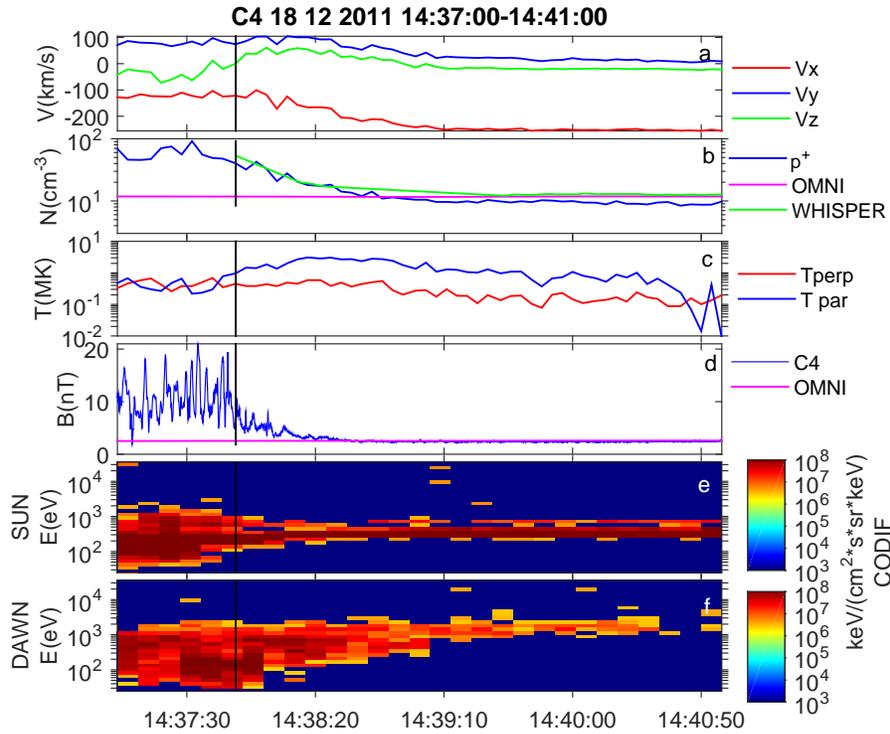
Figure 6. Overview of C4 magnetic and plasma (CODIF) measurements for event 18 December 2011. (a) proton velocity, (b) proton density, OMNI solar wind density, WHISPER electron density, (c) proton parallel and perpendicular temperature, (d) magnetic field magnitude and OMNI IMF magnitude, (e,f) proton spectrograms for the sunward and dawnward looking sectors.

3.2 Event 2

A shock from January 4th, 2008 (16:00–16:04 UT) was registered with Cluster C3 and C4 separation about 40 km. General event parameters are in Table S1, the overview of plasma and magnetic field parameters is in Fig.S1 in Supplement. The detailed wave activity at the front is presented in Fig. 10. Solar wind parameters and general crossing structure are very similar to that for Event 1. Solar wind speed is small ∼315 km/s, IMF magnitude — 2.4 nT. Alfvén Mach number is ≈23, magnetosonic
5   Mach number is ≈7, β (according to 1-min OMNI) is 12.2. Solar wind magnetic field measured locally by Cluster is the same as OMNI data (compare two lines in Fig. S1d), therefore OMNI β value is confirmed. All variants for θ_{Bn} give ∼40°.

The transition lasts about 2 minutes 16:00:50-16:02:50 from the first signs of gyrating ions upstream to the stable downstream conditions (Fig. S1f). The jump in magnetic field magnitude and ion density is smeared within half a minute 16:01:30-16:02:00 UT, and is wavy rather than step-like, downstream magnetic magnitude is often as small as 2–5 nT. The nominal shock front transition is somewhat arbitrarily placed at 16:01:35 UT at a first extended peak of magnetic field.
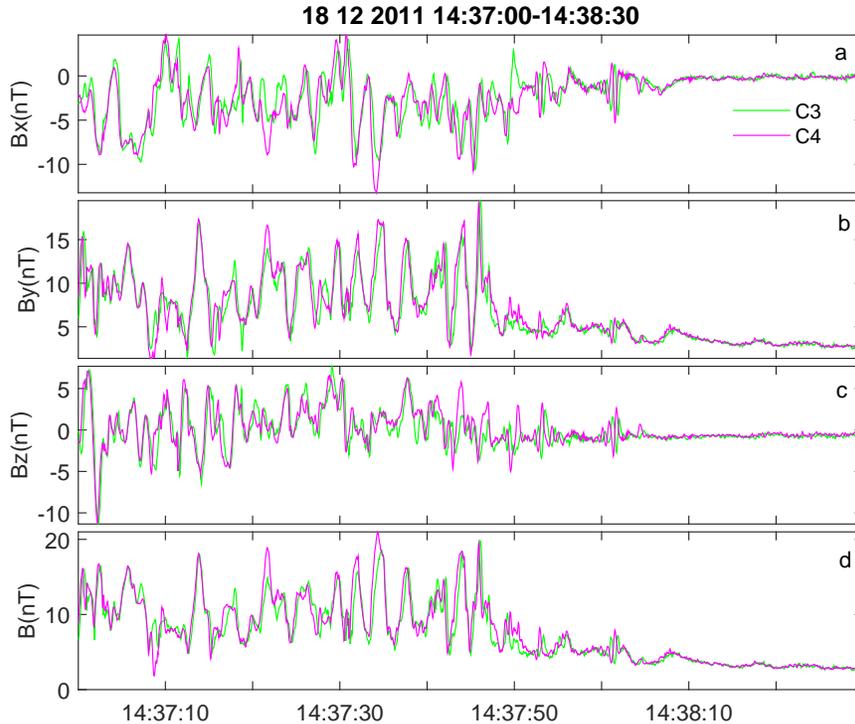
10

18 12 2011 14:37:00-14:38:30

Figure 7. Full resolution magnetic waveform for shock 18 December 2011. In panels (a-d) are components and total value of magnetic field.

Similar to Example 1, one can estimate shock speed along the normal, comparing with C2 crossings (not shown here). However for this example, the spacecraft separation is more than 11000 km, while the separation along the model normal is much smaller, just about 100 km. The estimated shock speed is 1.5–2.2 km/s (comparing the pairs C3-C2 and C4-C2), corresponding to the smeared ramp width about 50 km. However this estimate is very unreliable, since this calculation result would strongly depend on small variations of the actual normal.

The full resolution waveform is in Figure 10. Similar to Event 1, there is a dominating oscillation with the frequency about 0.4–0.5 Hz, as well as the lower amplitude waves with the frequency above 1 Hz (Fig. S2). **The specific feature of this event is an ultimate difference of C3 and C4 variations during the first 20 s downstream the front (16:01:25–16:01:35 UT), despite relatively small separation. The substantial difference in waveforms remains also further downstream. This specifics of variations typical for all shocks registered during this day (8 crossings within 2 hours in Table S1).**

Despite these differences, it is possible to perform multipoint separation analysis for the interval 16:01:15-16:01:25, where two waveforms in B_y component (Fig. 10b) are kind of similar and shifted by a fraction of period. All wave parameters (filtered in the range 0.1–2 Hz) are in Table 2. As in Event 1, maximum eigenvector is almost along Y, medium eigenvector — along X. Ratios of eigenvalues are $\lambda_{min}/\lambda_{int} = 0.15$, $\lambda_{int}/\lambda_{max} \approx 0.5$, thus the minimum variance (nominal propagation)
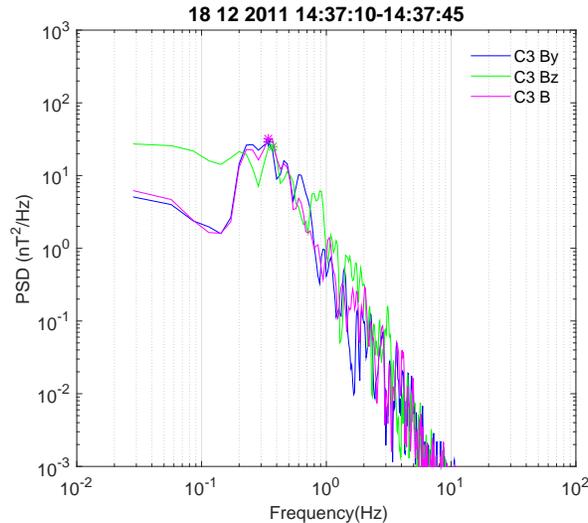
11

Figure 8. C3 frequency spectra for B_y, B_z components and magnetic field magnitude for shock 18 December 2011.

direction is well defined. The time shift between the magnetic measurements along the maximum variance component is 0.22 s (determined with correlation analysis), while the spacecraft separation along the minimum variance direction is 6.8 km. The resulting wavelength estimate is 61 km for the peak frequency 0.5 Hz. This value is close to spacecraft separation distance (about 40 km) and thus is generally consistent with the observed substantial difference between magnetic fields at C3 and C4.

The hodograph of magnetic field rotation (Fig. 11), however, shows absence of any stable polarization, which can be interpreted as sometimes linear, sometimes circular. The coplanarity approach again can not be used here to confirm the wave vector direction since the angle between the maximum variance direction and the local magnetic field is rather small (20°). The maximum possible wavelength (if spacecraft separation along wave vector is maximal 40 km) is $\sim$400 km.

3.3 Event 3

One more example is from January 3rd, 2008 (14:30–1435 UT) with Cluster separation $\sim$100 km (Table S1, Fig. S3 in Supplement). OMNI data showed very low IMF (1.1 nT) and $\beta = 39$. Solar wind speed is small $\sim$321 km/s, Alfvén Mach number is $\approx$42, magnetosonic Mach number is $\approx$7. The model θ_{Bn} is 47°. In Fig. 12 we present a view of local magnetic field along with OMNI data. Though local upstream magnitude is approximately equal to that in OMNI (except starting from 14:30 UT closer to the shock), the upstream field direction is changing by more than 90° and the local model θ_{Bn} is also changing to more perpendicular geometry. The presence of an earlier shock crossing at 14:20 UT may also affect observed upstream conditions. Downstream magnetic field is also strongly changing direction with a temporal scale of about a minute (Fig.12, right side). Therefore for this shock reliable determination of magnetic geometry is impossible. This problem may be inherently related with very small value of upstream magnetic field.
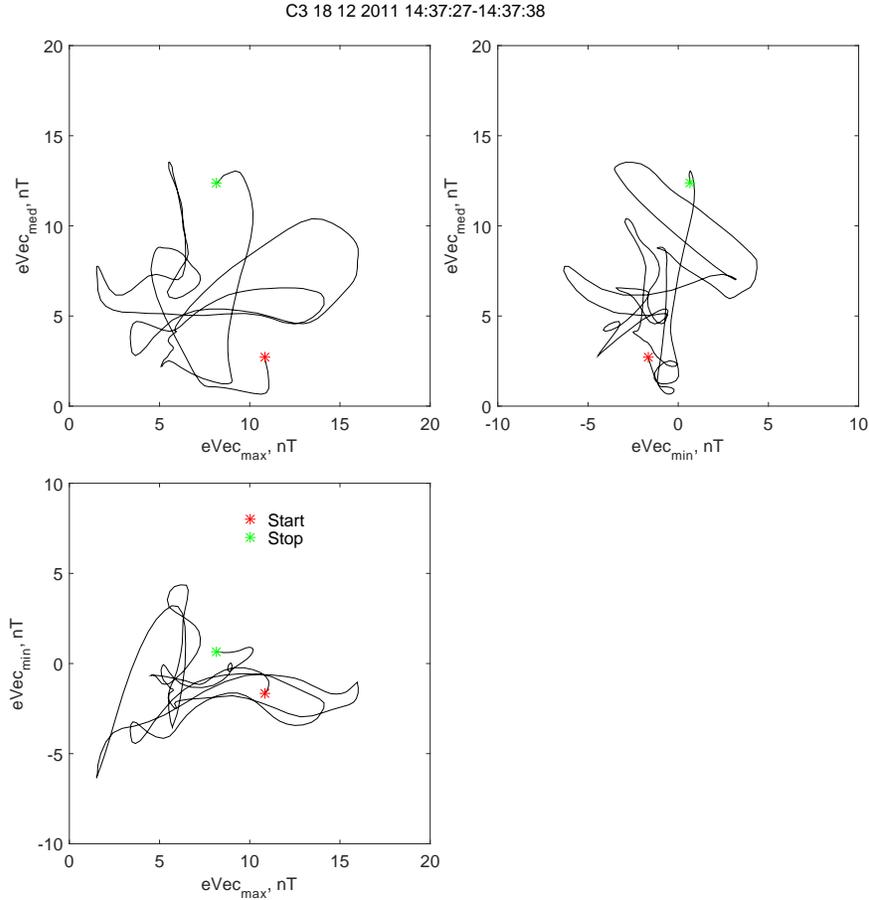
Figure 9. Hodographs of C3 magnetic field in eigenvector coordinates for shock 18 December 2011.

Fig. S3 contains overview of magnetic field and plasma parameters. The transition lasts about 2.5 minutes 14:32:00–14:34:30 from the first signs of gyrating ions upstream and growth of parallel ion temperature (Fig. S3e,f) to stable downstream conditions. The jump in magnetic field magnitude is smeared within half a minute 14:34:00–14:34:30 UT, it is wavy rather than step-like and magnetic magnitude downstream is often as small as 1–2 nT. The nominal shock front transition is somewhat arbitrarily placed at 14:34:10 UT (marked by vertical line in Fig.S3). Some increase of variation amplitudes around 14:34:10 can be interpreted as a localized front intensification or as a result of shock bounce motion.

Similar to Example 1, one can estimate shock speed along the normal, comparing with C2 crossing (not shown here). The spacecraft separation is 5700–5800 km, while the separation along the model normal is 1400 km. The estimated
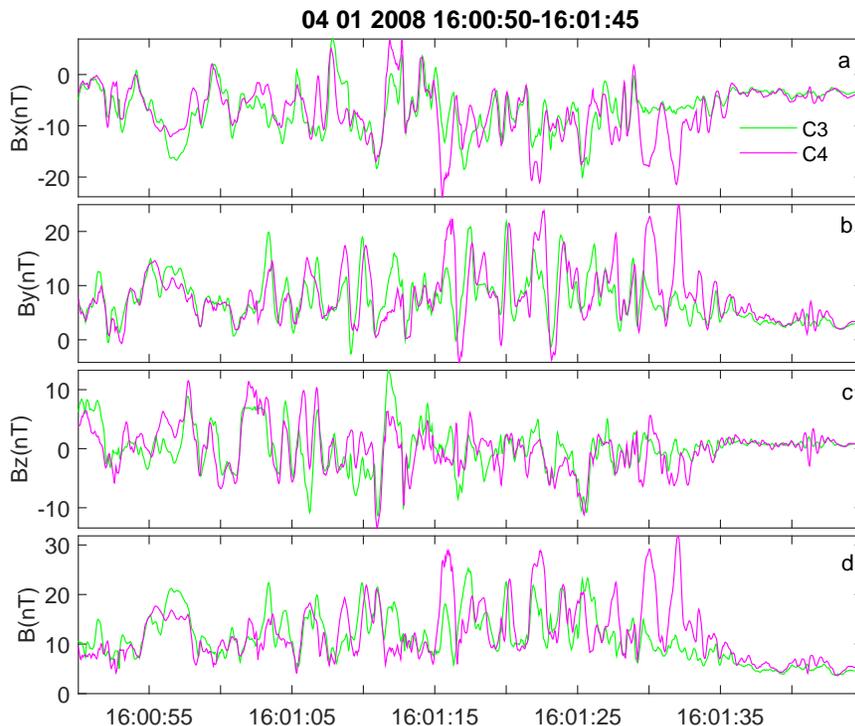
Figure 10. Full resolution magnetic waveform for shock 04 January 2008. In panels (a-d) are components and total value of magnetic field

shock speed is 11 km/s, corresponding to the smeared ramp width about 330 km. The gyroradius of solar wind protons is about 2000 km, the proton inertial length in solar wind is about 80 km.

The detailed view of magnetic variations is in Fig. 13. Only relatively high frequency oscillations about 2 Hz are present (frequency spectra are in Fig. S4). There are no wave packets with the stable phase. For example, at 14:34:10–14:34:14 UT X and Z components are in anticorrelation for C3 and C4, while immediately near, at 14:34:08–14:34:10 UT these components are in phase. Therefore, the reliable multipoint analysis for this event is impossible. Magnetic field hodograph plot for 14:34:10–14:34:14 is in Fig.14. It confirms unstable (but consistent with the changing linear) polarization. However, assuming that C3 and C4 variations are mostly in antiphase (half a period between spacecraft), one gets the maximal wavelength estimate $\sim$200 km.

3.4 Observation summary and statistics

Our statistics includes 22 oblique and quasi-perpendicular shocks. The three examples well illustrate typical shock properties. The minimum θ_{Bn} is 37°, two largest ones are 62° and 83°. Values of β range from 39 to 7.5. All cases are supercritical shocks with magnetosonic Mach number more than 5.5. Alfvén Mach numbers are large because of large β. All shocks exhibit
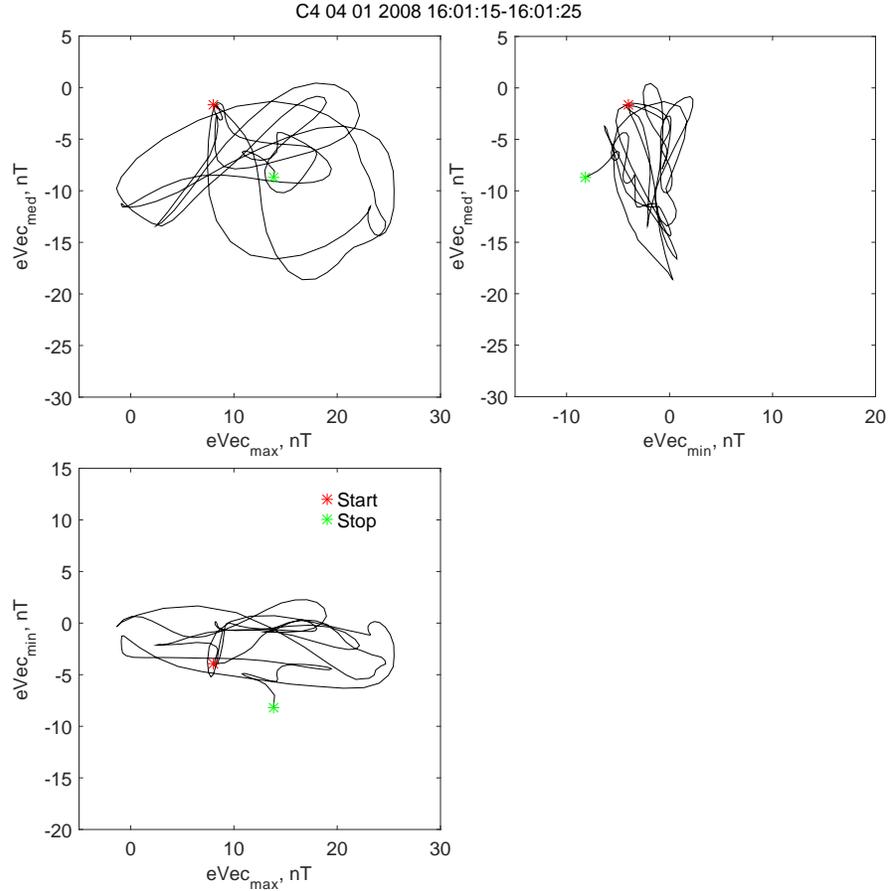
14

Figure 11. Hodographs of C4 magnetic field in eigenvector coordinates for shock 04 January 2008.

5 a clear several-minute-long transition zone between pristine solar wind ion flow and magnetosheath. The observed shocks, as concerns their general structure, are typical oblique/quasi-perpendicular shocks, with the somewhat smeared main magnetic field and density increase, which is **about several tens sec long or several hundred km.** This magnetic profile is typical for all our shocks irrespective of θ_{Bn} angle.

On a smaller time scale of seconds, the magnetic profile is dominated by very large amplitude magnetic variations much

10 larger than the background field, which are gradually growing in the course of magnetic field increase towards downstream. As a result, the exact location of the 'main' magnetic jump (aka ramp for supercritical quasi-perpendicular shocks) can not be defined. This presence of high-amplitude variations is in agreement with the previous publications (Winterhalter and Kivelson, 1988).

15

Table 2. Wave analysis data for shock 04 January 2008, 16:01:15–16:01:25.

max eigenvector, V_{max}	-0.46 0.87 0.17
med eigenvector, V_{med}	0.88 0.42 0.22
min eigenvector, V_{min}	-0.12 -0.25 0.96
eigenvalues	3.4, 22.9, 45.3
magnetic field C3, B_3 (nT)	-9.05, 9.85, -0.75
local proton velocity C4 (km/s)	-178.3, 125.7, -67.4
angle, V_{max} and IMF	46°
angle, V_{min} and IMF	79°
angle, V_{max} and B_3	20°
angle, V_{min} and B_3	99°
peak frequency in max component	0.5 Hz
time shift in magnetic field along V_{max}	0.22 s
separation along V_{min}	6.8 km
wavelength	61 km

The three examples show characteristics of the dominating magnetic variations, typical for all considered events. The detailed multipoint variation analysis allowed to obtain following new information. In the most of shocks (and in Examples 1 and 2) the variations exhibit the well defined frequency peak $\sim$0.2–0.5 Hz. The magnetic phase portrait of these variations is irregular, with no clear persistent polarization. It can be also interpreted as a linear polarization with the frequently changing main direction. However since amplitude of variations is larger than the background field, the main axis of linear polarization is always almost along the field vector. Such polarization does not allow to determine reliably the wave propagation direction and the wavelength. We get the estimates only in the range several-tens-hundreds km.

Two shock events (Dec. 31, 2003 and our Example 3, Jan. 3, 2008 14:32 UT) have dominating $\sim$2 Hz variations, visually with more harmonic waveform, but also with the unstable phase. The spatial scale of these variations is smaller than the spacecraft separation, so that it proved to be impossible to determine it with multipoint data. These two shocks are not different from the other events in terms of their other general parameters. Moreover one of them (Event 3 above) is registered just 10 min after a crossing, which exhibited the first type of variations. Therefore the presence of '2-Hz' waves might be due to some temporal shock front evolution.
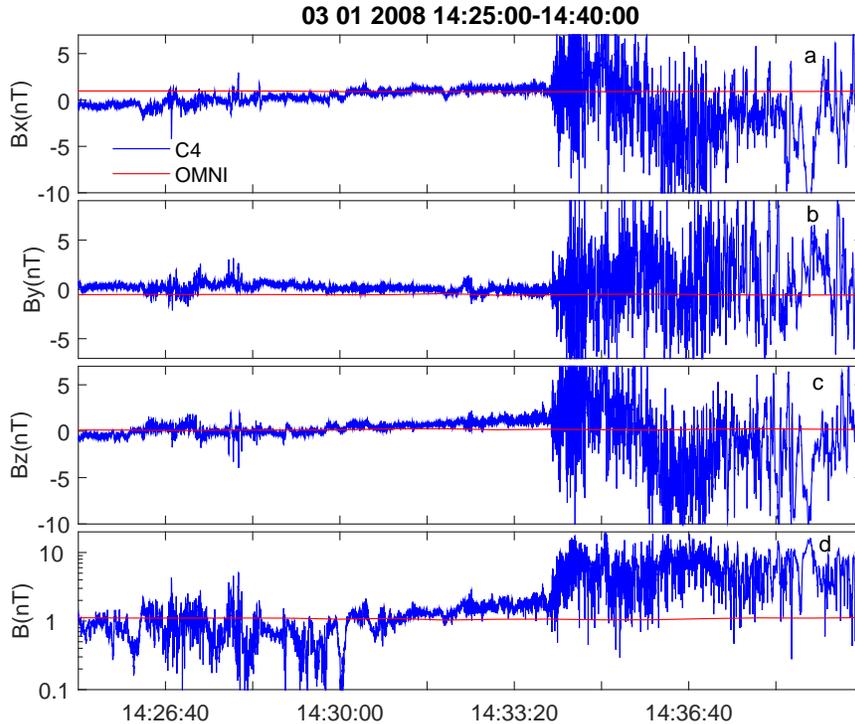
Figure 12. Local upstream and OMNI magnetic field for shock 03 January 2008. In panels (a-d) are components and total value of magnetic field

4 Discussion

4.1 Reliability of solar wind input

High-β solar wind is relatively rare at the Earth orbit. In our study we accepted somewhat ad-hoc threshold of high β equal to 10. Such interplanetary conditions tend to occur during solar minima, being created by slow cold dense solar wind with low IMF (1–2 nT). However is not always easy to confirm that the observed shock crossing actually occurred in high-β solar wind interval, identified in OMNI. The first set of problems is related with association of particular crossings with the stable high β. These problems are relatively straightforward to identify in data. A more substantial problem is related with the inherent solar wind and IMF variability. We measure solar wind in L1 halo orbit, 1.5 million kilometers away from Earth and with halo radius not less than 200 000 km (for ACE spacecraft). A substantial part of modern OMNI data are taken from Wind spacecraft, which is currently on a much wider halo orbit (300–400 thousand km) (Podladchikova et al., 2018). Solar wind and IMF structures at L1 are not necessarily the same, that actually affect the magnetosphere. The most questionable is spatial persistence of relatively small changes of IMF from 2 to 1 nT, responsible for creation of very high-β intervals.
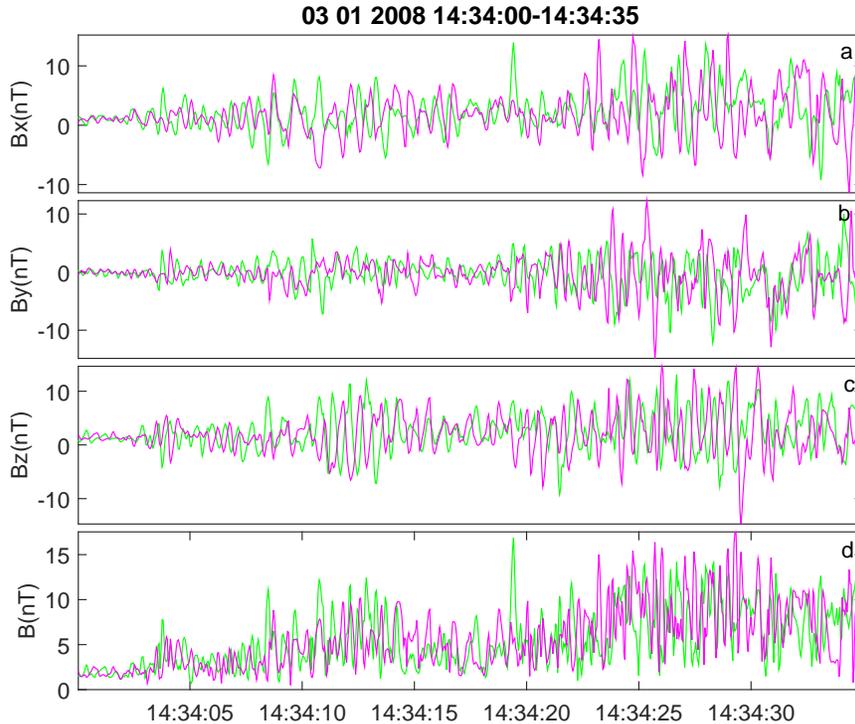
17

Figure 13. Full resolution magnetic waveform for shock 03 January 2008. In panels (a-d) are components and total value of magnetic field

Though the specific analysis of the spatial scales of high-β areas in solar wind was not performed, available reports indicate

15 significant potential problems. The ISEE data study suggested that during periods of medium to low variance of magnetic field, magnetic features with the scales about 20 R_E perpendicular to the IMF may occur (Crooker et al., 1982). Comparison of L1 Wind and near-Earth Interball data for 1996–1999 have shown (Petrukovich et al., 2001), that the IMF structures, associated with geomagnetic storms (with the threshold of IMF B_z GSM below –10 nT during 3 hours) are practically the same in L1 and the near-Earth orbits. However, about 20–80% of the smaller everyday IMF variations, causing substorms (several nT in

20 magnitude on one-hour scale) are different by more than 25%.

Thus very high β values in OMNI are not readily applicable for a shock study. It is not always possible to check solar wind β immediately before shock crossing. A spacecraft needs to probe pristine solar wind and then rapidly cross the shock, or there should be an additional near-Earth solar wind monitor. Magnetic field can be reliably measured with magnetometer (still assuming offset uncertainty of about 0.1 nT). Accuracy of ion density and temperature measurements is more problematic,

25 since at L1 the specialised thoroughly calibrated instruments are used, while with a magnetospheric spacecraft, calibration could be rougher in solar wind. Assumptions on the constant helium content and constant electron temperature, used while OMNI β calculations, may also result in some errors. **For example, a factor of two change in electron temperature will**
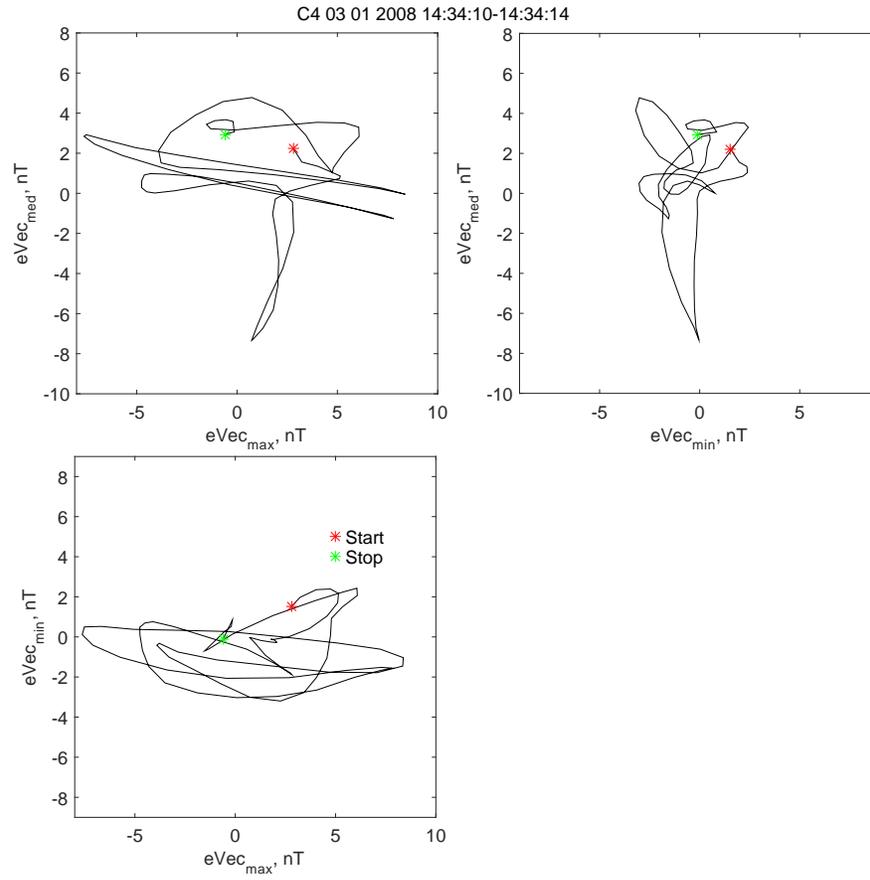
18

Figure 14. Hodographs of C4 magnetic field in eigenvector coordinates for shock 03 January 2008 for 14:34:10-14:34:14.

result in the change of β by about 30%. Factor of two variations of the He++ content will result in variations of β around 10%. Of course, an additional (relative to those found in the OMNI set) high β intervals may actually form near the bow shock, as a side product of such variability.

4.2 Shock properties

Rather compact large-scale structure of the observed shock transitions is similar to that reported for oblique and quasi perpendicular shocks. It is distinctly different from the structure of quasi-parallel shocks, which are extended up to several Earth radii. However, there are some differences with low-β shocks on a smaller scale. For example the main magnetic and ion density increase in the shock front for all observed events was around several tens of seconds or several hundred km. This scale is larger, than proton inertial length, but smaller than ion gyroradius in solar wind. Dependence of shock spatial scale on β is an interesting moment and should be addressed in future studies on larger statistics.

Magnetic variations appear during this ramp-like increase and have the amplitude comparable or larger than the background magnetic field, so that there is no 'stable' magnetic structure on the time scales of seconds. In comparison, for a supercritical quasi-perpendicular low-β shock, one usually defines, starting from the upstream, the prolonged interval of somewhat enhanced density and magnetic field (shock foot, lasting tens of seconds) and the sharp main increase (ramp, lasting seconds). The ramp is often used to determine the shock motion with multipoint measurements, but in our case it is impossible. The increased width of main magnetic jump and its wavy nature might be related with some essential scales in the high-β plasma (large ion gyro radius) or be a sign of an unstable cyclically reforming shock (e.g., Lefebvre et al., 2009). A more detailed phenomenological description of this shock transition requires analysis of ion kinetics, which will be performed elsewhere.

Observed shock crossings in their general appearance, in particular, with the presence of high-amplitude magnetic variations and absence of clear ramp profile, are similar to those earlier presented by Formisano et al. (1975) and Farris et al. (1992) (as far as it can be discerned with visual examination of figures). In this study we advance our knowledge, determining some quantitative features of those variations.

4.3 Magnetic variation properties

Observed properties of low-frequency magnetic variations (linear polarization with very high amplitude, substantially changing the total magnetic field) suggest their strong non-linearity and compressive nature. Absence of any several-periods-long wave packets with the stable phase also suggest strong spatial localisation.

With two Cluster spacecraft separated by several tens km it was possible to estimate the spatial scale of these dominating variations. Three typical variants were found. In some events (Example 1) variations had rather irregular form, typical frequency of about 0.5 Hz, and were very similar on two spacecraft, suggesting the scale of some hundred km. The wavelength can be determined in dependently to propagation direction only with four measuring points, unlike our cases. Alternatively one can fix propagation direction with the minimum variance analysis in the case of elliptic polarization or with the coplanarity supposition. Unfortunately in our cases it proved to be impossible to determine

the wavevector direction reliably by both methods, since we have linearly polarized waves with maximum variance direction along the main magnetic field. Note, that such configuration is inevitable for a variation much larger than the background field.

30   The second variant of a spatial scale is illustrated with Example 2. It includes the variations visually similar to that in Example 1, but with a mix of scales of the order of hundred km, which can be captured with our spacecraft separation, and of the order of tens km. As a result, the waveforms are rather different, but common features can sometimes be traced. Finally, the third variant (Example 3) contains more harmonic waves with higher frequencies around 1–2 Hz and the unresolved dominating spatial scale of at most 200 km.

The observed variations are strongly different from that in low-β supercritical events (e.g. Krasnoselskikh et al., 2013), where clear whistler wave packets with elliptic polarization dominate. Observed polarization is also not consistent with the Alfvén mode, earlier suggested for high-β shock (Coroniti, 1970; Kennel and Sagdeev, 1967).

Dominating downstream wave mode was also addressed in a number of other investigations, however cases of re-
5   ally high $\beta > 10$ were not specifically addressed. Hubert et al. (1989) identified the mirror waves, comparing magnetic field with density, provided by the fast electron measurements of ISEE project. Balikhin et al. (1997) identified the intermediate mode with two-point AMPTE data analysis. Lacombe et al. (1992) suggested for higher-β shocks the mirror mode with linear polarization, and successfully used coplanarity assumption to define the wavevector direction. Czaykowska et al. (2001) have shown compressive mode as well as left-hand polarized mode in shocks with $\beta > 1$.
10   Therefore, almost full variety of possible wave mode variants was identified. A definite plasma mode analysis critically depends on reliable determination of the wave propagation (wavevector) direction, which proved to be impossible in our cases. Also, it should be noted, that all studies referenced above, used several-minute data intervals, which were often several minutes away from the shock transition. In the most of cases, the analysed frequencies were below 0.1 Hz. This approach is different from ours, we addressed relatively short intervals of the most powerful oscillations.

15   Though some of the above-cited studies addressed 'higher-β' shocks, actually their statistics was definitely dominated with $\beta \geq 1$ cases. The only published cases with really high β (Formisano et al., 1975; Winterhalter and Kivelson, 1988; Farris et al., 1992) were not accompanied with any plasma mode analysis, however visually the wave actitvity in these events were similar to our Examples 1 and 2.

An alternative wave mode candidate, frequently suggested for high-β plasma, is Weibel instability, which is funda-
20   mentally similar to drift mirror mode. With no seed magnetic field the Weibel mode has only imaginary frequency. The latter means that the magnetic field clamps are growing faster, than propagate. For finite magnetic field Pokhotelov and Balikhin (2012) suggested, that Weibel mode grows as a mix of two opposite circular polarizations, attains some small real part of frequency. Thus in some features (linear polarization, chaotic phase) it is consistent with observations.

5   Conclusions

High-β ($\beta > 10$) shocks are relatively rare and largely unexplored class of Earth bow shock. Formation of high-β interplanetary plasmas is mostly related with dense slow solar wind and very low magnetic field up to 1–2 nT. **Due to spatial variability of low IMF, it is more difficult to determine shock geometry for higher β (in OMNI) cases. However at some (large) β shock structure should become independent from magnetic field direction. This is an interesting direction of future studies.**

Our statistics includes oblique and quasi-perpendicular shocks. The main magnetic field and ion density jumps in the shock fronts are smeared to several hundred km, so the overall layout is quite characteristic and distinctly different from that for quasi-parallel and supercritical quasi-perpendicular shocks.

Dominating magnetic variations have amplitudes much larger than the background field, frequencies 0.2–0.5 Hz, sometimes, $\sim$2 Hz. Polarization is mostly irregular and close to linear, the spatial scales range from several tens to couple hundred km. These properties are definitely different from that for fast magnetosonic or Alfvén modes earlier reported for some other shock types. In some features the variations may be consistent with the Weibel instability, but observations with more closely spaced spacecraft are necessary to conclude more definitely on the wave mode.

References

10 Axford, W. I., Leer, E., and Skadron, G.: The Acceleration of Cosmic Rays by Shock Waves, International Cosmic Ray Conference, 11, 132, 1977.

Balikhin, M., Gedalin, M., and Petrukovich, A.: New mechanism for electron heating in shocks., , 70, 1259–1262, https://doi.org/10.1103/PhysRevLett.70.1259, 1993.

Balikhin, M. A., Woolliscroft, L. J. C., Alleyne, H. S. C., Dunlop, M., and Gedalin, M. A.: Determination of the disper-
15 sion of low frequency waves downstream of a quasiperpendicular collisionless shock, Annales Geophysicae, 15, 143–151, https://doi.org/10.1007/s00585-997-0143-x, 1997.

Balogh, A., Carr, C. M., Acuña, M. H., Dunlop, M. W., Beek, T. J., Brown, P., Fornaçon, K. H., Georgescu, E., Glassmeier, K. H., Harris, J., Musmann, G., Oddy, T., and Schwingenschuh, K.: The Cluster Magnetic Field Investigation: overview of in-flight performance and initial results, Annales Geophysicae, 19, 1207–1217, https://doi.org/10.5194/angeo-19-1207-2001, 2001.

20 Burgess, D., Lucek, E. A., Scholer, M., Bale, S. D., Balikhin, M. A., Balogh, A., Horbury, T. S., Krasnoselskikh, V. V., Kucharek, H., Lembège, B., Möbius, E., Schwartz, S. J., Thomsen, M. F., and Walker, S. N.: Quasi-parallel Shock Structure and Processes, , 118, 205–222, https://doi.org/10.1007/s11214-005-3832-3, 2005.

Coroniti, F. V.: Turbulence structure of high-β perpendicular fast shocks, Journal of Geophysical Research, 75, 7007, https://doi.org/10.1029/JA075i034p07007, 1970.

25 Crooker, N. U., Siscoe, G. L., Russell, C. T., and Smith, E. J.: Factors controlling degree of correlation between ISEE 1 and ISEE 3 interplanetary magnetic field measurements, Journal of Geophysical Research, 87, 2224–2230, https://doi.org/10.1029/JA087iA04p02224, 1982.

Czaykowska, A., Bauer, T. M., Treumann, R. A., and Baumjohann, W.: Magnetic field fluctuations across the Earth's bow shock, Annales Geophysicae, 19, 275–287, https://doi.org/10.5194/angeo-19-275-2001, 2001.

30 Dimmock, A. P., Balikhin, M. A., Walker, S. N., and Pope, S. A.: Dispersion of low frequency plasma waves upstream of the quasi-perpendicular terrestrial bow shock, Annales Geophysicae, 31, 1387–1395, https://doi.org/10.5194/angeo-31-1387-2013, 2013.

Donnert, J., Vazza, F., Brüggen, M., and ZuHone, J.: Magnetic Field Amplification in Galaxy Clusters and Its Simulation, , 214, 122, https://doi.org/10.1007/s11214-018-0556-8, 2018.

Farris, M. H., Petrinec, S. M., and Russell, C. T.: The thickness of the magnetosheath: Constraints on the polytropic index, Geophysical
35 Research Letters, 18, 1821–1824, https://doi.org/10.1029/91GL02090, 1991.

Farris, M. H., Russell, C. T., Thomsen, M. F., and Gosling, J. T.: ISEE 1 and 2 observations of the high beta shock, Journal of Geophysical Research, 97, 19 121–19 127, https://doi.org/10.1029/92JA01976, 1992.

Formisano, V., Russell, C. T., Means, J. D., Greenstadt, E. W., Scarf, F. L., and Neugebauer, M.: Collisionless shock waves in space: A very high β structure, Journal of Geophysical Research, 80, 2013, https://doi.org/10.1029/JA080i016p02013, 1975.

5 Hobara, Y., Balikhin, M., Krasnoselskikh, V., Gedalin, M., and Yamagishi, H.: Statistical study of the quasi-perpendicular shock ramp widths, Journal of Geophysical Research (Space Physics), 115, A11106, https://doi.org/10.1029/2010JA015659, 2010.

Hubert, D., Perche, C., Harvey, C. C., Lacombe, C., and Russell, C. T.: Observation of mirror waves downstream of a quasi-perpendicular shock, Geophysical Research Letters, 16, 159–162, https://doi.org/10.1029/GL016i002p00159, 1989.

Hubert, D., Lacombe, C., Harvey, C. C., Moncuquet, M., Russell, C. T., and Thomsen, M. F.: Nature, properties, and origin of low-frequency waves from an oblique shock to the inner magnetosheath, Journal of Geophysical Research, 103, 26 783–26 798, https://doi.org/10.1029/98JA01011, 1998.

Kennel, C. F. and Sagdeev, R. Z.: Collisionless shock waves in high β plasmas: 1, Journal of Geophysical Research, 72, 3303–3326, https://doi.org/10.1029/JZ072i013p03303, 1967.

Kennel, C. F., Edmiston, J. P., and Hada, T.: A quarter century of collisionless shock research, Washington DC American Geophysical Union Geophysical Monograph Series, 34, 1–36, https://doi.org/10.1029/GM034p0001, 1985.

Krasnoselskikh, V., Balikhin, M., Walker, S. N., Schwartz, S., Sundkvist, D., Lobzin, V., Gedalin, M., Bale, S. D., Mozer, F., Soucek, J., Hobara, Y., and Comisel, H.: The Dynamic Quasiperpendicular Shock: Cluster Discoveries, , 178, 535–598, https://doi.org/10.1007/s11214-013-9972-y, 2013.

Krasnoselskikh, V. V., Lembège, B., Savoini, P., and Lobzin, V. V.: Nonstationarity of strong collisionless quasiperpendicular shocks: Theory and full particle numerical simulations, Physics of Plasmas, 9, 1192–1209, https://doi.org/10.1063/1.1457465, 2002.

Krymskii, G. F.: A regular mechanism for the acceleration of charged particles on the front of a shock wave, Soviet Physics Doklady, 22, 327, 1977.

Lacombe, C., Pantellini, F. G. E., Hubert, D., Harvey, C. C., Mangeney, A., Belmont, G., and Russell, C. T.: Mirror and Alfvenic waves observed by ISEE 1-2 during crossings of the earth's bow shock, Annales Geophysicae, 10, 772–784, 1992.

Lefebvre, B., Seki, Y., Schwartz, S. J., Mazelle, C., and Lucek, E. A.: Reformation of an oblique shock observed by Cluster, Journal of Geophysical Research (Space Physics), 114, A11107, https://doi.org/10.1029/2009JA014268, 2009.

Markevitch, M. and Vikhlinin, A.: Shocks and cold fronts in galaxy clusters, , 443, 1–53, https://doi.org/10.1016/j.physrep.2007.01.001, 2007.

Petrukovich, A. A., Romanov, S. A., and Klimov, S. L.: Direct Measurements of AC Plasma Currents in the Outer Magnetosphere, Washington DC American Geophysical Union Geophysical Monograph Series, 103, 199, https://doi.org/10.1029/GM103p0199, 1998.

Petrukovich, A. A., Klimov, S. I., Lazarus, A., and Lepping, R. P.: Comparison of the solar wind energy input to the magnetosphere measured by Wind and Interball-1, Journal of Atmospheric and Solar-Terrestrial Physics, 63, 1643–1647, https://doi.org/10.1016/S1364-6826(01)00039-6, 2001.

Podladchikova, T., Petrukovich, A., and Yermolaev, Y.: Geomagnetic storm forecasting service StormFocus: 5 years online, Journal of Space Weather and Space Climate, 8, A22, https://doi.org/10.1051/swsc/2018017, 2018.

Pokhotelov, O. A. and Balikhin, M. A.: Weibel instability in a plasma with nonzero external magnetic field, Annales Geophysicae, 30, 1051–1054, https://doi.org/10.5194/angeo-30-1051-2012, 2012.

Rème, H., Aoustin, C., Bosqued, J. M., Dandouras, I., Lavraud, B., Sauvaud, J. A., Barthe, A., Bouyssou, J., Camus, T., Coeur-Joly, O., Cros, A., Cuvilo, J., Ducay, F., Garbarowitz, Y., Medale, J. L., Penou, E., Perrier, H., Romefort, D., Rouzaud, J., Vallat, C., Alcaydé, D., Jacquey, C., Mazelle, C., D'Uston, C., Möbius, E., Kistler, L. M., Crocker, K., Granoff, M., Mouikis, C., Popecki, M., Vosbury, M., Klecker, B., Hovestadt, D., Kucharek, H., Kuenneth, E., Paschmann, G., Scholer, M., Sckopke, N., Seidenschwang, E., Carlson, C. W., Curtis, D. W., Ingraham, C., Lin, R. P., McFadden, J. P., Parks, G. K., Phan, T., Formisano, V., Amata, E., Bavassano- Cattaneo, M. B., Baldetti, P., Bruno, R., Chionchio, G., di Lellis, A., Marcucci, M. F., Pallocchia, G., Korth, A., Daly, P. W., Graeve, B., Rosenbauer, H., Vasyliunas, V., McCarthy, M., Wilber, M., Eliasson, L., Lundin, R., Olsen, S., Shelley, E. G., Fuselier, S., Ghielmetti, A. G., Lennartsson, W., Escoubet, C. P., Balsiger, H., Friedel, R., Cao, J. B., Kovrazhkin, R. A., Papamastorakis, I., Pellat, R., Scudder, J., and Sonnerup,

B.: First multispacecraft ion measurements in and near the Earth's magnetosphere with the identical Cluster ion spectrometry (CIS)
experiment, Annales Geophysicae, 19, 1303–1354, https://doi.org/10.5194/angeo-19-1303-2001, 2001.

Sagdeev, R. Z.: Cooperative Phenomena and Shock Waves in Collisionless Plasmas, Reviews of Plasma Physics, 4, 23, 1966.

Schwartz, S. J., Henley, E., Mitchell, J., and Krasnoselskikh, V.: Electron Temperature Gradient Scale at Collisionless Shocks, , 107, 215002,
https://doi.org/10.1103/PhysRevLett.107.215002, 2011.

Scudder, J. D., Mangeney, A., Lacombe, C., Harvey, C. C., Aggson, T. L., Anderson, R. R., Gosling, J. T., Paschmann, G., and Russell, C. T.:
The resolved layer of a collisionless, high β, supercritical, quasi-perpendicular shock wave 1. Rankine- Hugoniot geometry, currents, and
stationarity, Journal of Geophysical Research, 91, 11 019–11 052, https://doi.org/10.1029/JA091iA10p11019, 1986.

Vasko, I. Y., Mozer, F. S., Krasnoselskikh, V. V., Artemyev, A. V., Agapitov, O. V., Bale, S. D., Avanov, L., Ergun, R., Giles, B., Lindqvist,
P. A., Russell, C. T., Strangeway, R., and Torbert, R.: Solitary Waves Across Supercritical Quasi-Perpendicular Shocks, Geophysical
Research Letters, 45, 5809–5817, https://doi.org/10.1029/2018GL077835, 2018.

Walker, S., Alleyne, H., Balikhin, M., André, M., and Horbury, T.: Electric field scales at quasi-perpendicular shocks, Annales Geophysicae,
22, 2291–2300, https://doi.org/10.5194/angeo-22-2291-2004, 2004.

Wilson, Lynn B., I., Stevens, M. L., Kasper, J. C., Klein, K. G., Maruca, B. A., Bale, S. D., Bowen, T. A., Pulupa, M. P., and Salem,
C. S.: The Statistical Properties of Solar Wind Temperature Parameters Near 1 au, The Astrophysical Journal Supplement Series, 236, 41,
https://doi.org/10.3847/1538-4365/aab71c, 2018.

Winterhalter, D. and Kivelson, M. G.: Observations of the Earth's bow shock under high Mach number/high plasma beta solar wind condi-
tions, Geophysical Research Letters, 15, 1161–1164, https://doi.org/10.1029/GL015i010p01161, 1988.